

Rochester Institute of Technology

## RIT Digital Institutional Repository

---

Theses

---

5-2021

### A Programmable Processing-in-Memory Architecture for Memory Intensive Applications

Mark Connolly  
mfc5867@rit.edu

Follow this and additional works at: <https://repository.rit.edu/theses>

---

#### Recommended Citation

Connolly, Mark, "A Programmable Processing-in-Memory Architecture for Memory Intensive Applications" (2021). Thesis. Rochester Institute of Technology. Accessed from

This Thesis is brought to you for free and open access by the RIT Libraries. For more information, please contact [repository@rit.edu](mailto:repository@rit.edu).

---

# **A Programmable Processing-in-Memory Architecture for Memory Intensive Applications**

MARK CONNOLLY

---

---

# A Programmable Processing-in-Memory Architecture for Memory Intensive Applications

MARK CONNOLLY

May 2021

A Thesis Submitted  
in Partial Fulfillment  
of the Requirements for the Degree of  
Master of Science  
in  
Computer Engineering

**R·I·T** | KATE GLEASON  
*College of ENGINEERING*

*Department of Computer Engineering*

---

# A Programmable Processing-in-Memory Architecture for Memory Intensive Applications

MARK CONNOLLY

## Committee Approval:

---

Dr. Amlan Ganguly *Advisor*  
Department Head

Date

---

Mark Indovina  
Senior Lecturer

Date

---

Dr. Cory Merkel  
Assistant Professor

Date

## Abstract

While both processing and memory architectures are rapidly improving in performance, memory architecture is lagging behind. As performance of processing architecture continues to eclipse that of memory, the memory architecture continues to become an increasingly unavoidable bottleneck in computer architecture. There are two drawbacks that are commonly associated with memory accesses: i) large delays causing the processor to remain idle waiting on data to become available and ii) the power consumption required to transfer the data. These performance issues are especially notable in research and enterprise computing applications such as deep learning models. Even when data for an application such as this is transferred to a cache before processing to avoid the delay, the large power cost of the transfer is still incurred.

Processing-in-memory (PIM) architectures offer a solution to the issues in modern memory architecture. The inclusion of processing elements within the memory architecture reduces data transfers between the host processor and memory, thus reducing penalties incurred by memory accesses. The programmable-PIM (pPIM) architecture is a novel PIM architecture that delivers the performance enhancements of PIM while delivering a high degree of reprogrammability through the use of look-up tables (LUTs).

A novel instruction set architecture (ISA) for the pPIM architecture facilitates the architecture's reprogrammability without large impacts on performance. The ISA takes a microcoded approach to handling the control signals of the pPIM control signals. This approach allows variable-stage instructions at a low additional cost to the overall power and area of the architecture.

The versatility of the pPIM architecture enables MAC operations and several common activation functions to be modeled for execution on the architecture. As a measure of performance, post-synthesis models of both the pPIM architecture and the

ISA are generated for CNN inference. As a proof-of-concept an FPGA model of the pPIM architecture is developed for representations of a single layer neural network (NN) model for classification of MNIST images.

# Contents

---

Signature Sheet	i
Abstract	ii
Table of Contents	iv
List of Figures	vi
List of Tables	1
<b>1 Introduction</b>	<b>2</b>
1.1 Motivation . . . . .	2
<b>2 Background</b>	<b>5</b>
2.1 Processing-in-Memory . . . . .	5
2.2 Instruction Set Architectures . . . . .	7
2.3 Neural Networks . . . . .	8
2.4 Supporting Work . . . . .	10
<b>3 pPIM Architecture</b>	<b>11</b>
3.1 pPIM Core . . . . .	12
3.2 pPIM Cluster . . . . .	13
3.3 pPIM Function Word Generation . . . . .	14
3.4 pPIM MAC Operations . . . . .	14
3.5 pPIM Activation Operations . . . . .	17
3.6 FPGA Implementation . . . . .	20
3.6.1 Technology & Resources . . . . .	20
3.6.2 Machine Learning Model . . . . .	21
3.6.3 pPIM Implementation . . . . .	21
3.6.4 Communication . . . . .	22
3.7 Results . . . . .	23
3.7.1 pPIM Characteristics . . . . .	23
3.7.2 Performance Evaluation . . . . .	24
3.7.3 FPGA Characteristics . . . . .	26
3.7.4 FPGA Performance Evaluation . . . . .	27

<b>4</b>	<b>pPIM Instruction Set Architecture</b>	<b>28</b>
4.1	ISA Communication . . . . .	29
4.2	pPIM Microcode . . . . .	29
4.3	pPIM Instruction Formatting . . . . .	31
4.4	pPIM ISA Operation Mapping . . . . .	32
4.5	FPGA Implementation . . . . .	34
4.5.1	Technology & Resources . . . . .	34
4.5.2	ISA Implementation . . . . .	35
4.6	Results . . . . .	36
4.6.1	ISA Characteristics . . . . .	36
4.6.2	FPGA Characteristics . . . . .	38
<b>5</b>	<b>Conclusions &amp; Future Work</b>	<b>40</b>
5.1	Future Work . . . . .	41
	<b>Bibliography</b>	<b>42</b>



# List of Figures

---

1.1	The growing divide between processor speeds and memory bandwidth that leads to a throttling of processor performance [1] . . . . .	3
2.1	The various types of processing with respect to their interaction with memory. Traditional architectures include a cache coupled with processors. More recent architectures have attempted to reduce the distance of memory from the processing power to reduce delays with 'near memory' approaches. PIM goes a step beyond and introduces the processing power within the memory architecture for further reduced latencies[2].	6
3.1	Heirarchical view of the pPIM architecture . . . . .	11
3.2	Layout of the pPIM core architecture. . . . .	12
3.3	Layout of the pPIM cluster architecture. . . . .	13
3.4	Calculation of the result of an unsigned multiplication through the calculation and summation of partial products. . . . .	15
3.5	Model of dataflow within a pPIM cluster for both (a) 8-bit full precision and (b) 4-bit half precision unsigned MAC operations . . . . .	15
3.6	Calculation of the result of a signed multiplication through the calculation and summation of partial products. . . . .	16
3.7	Model of dataflow within a pPIM cluster for both (a) 8-bit full precision and (b) 4-bit half precision signed MAC operations . . . . .	17
3.8	Model of dataflow within a pPIM cluster for both (a) 16-bit precision and (b) 8-bit precision ReLu activation operations. . . . .	18
3.9	Model of dataflow within a pPIM cluster for both (a) 16-bit precision and (b) 8-bit precision saturated ReLu activation operations. . . . .	18
3.10	Configuration of a pPIM cluster for quick switching between activation operations. . . . .	19
3.11	Model of dataflow within a pPIM cluster for a 16-bit max-index operation. . . . .	19
3.12	Structure of the multiple region approach to designing an FPGA implementation of the pPIM architecture. . . . .	22
3.13	Communication model between multiple elements within the ZC702 evaluation board and the host CPU. . . . .	22

3.14	Comparison of various high-performance architectures on their throughput with popular deep learning models. . . . .	24
3.15	Layout of the pPIM cluster architecture. . . . .	25
3.16	Layout of the pPIM cluster architecture. . . . .	25
3.17	Predictions made by the pPIM architecture running on the ZC702 base board. . . . .	27
4.1	Proposed ISA for handling control signals and memory accesses of the pPIM architecture. . . . .	28
4.2	Model of interface between the ISA with pPIM Clusters and memory elements. . . . .	29
4.3	ISA . . . . .	30
4.4	Formatting of instruction sent from host CPU to pPIM ISA. . . . .	31
4.5	Timing example of two consecutive MAC operations performed on a pPIM cluster by the pPIM ISA. . . . .	34
4.6	Timing example of two consecutive MAC operations performed on a pPIM cluster by the pPIM ISA. . . . .	35
4.7	Comparison of power consumption of the ISA and pPIM clusters in various deep learning models. . . . .	37
4.8	Comparison of throughput for inference on Alexnet. . . . .	38

## List of Tables

---

3.1	Synthesis results for pPIM architecture. . . . .	23
3.2	Synthesis results for FPGA implementation . . . . .	26
3.3	Timing results for FPGA implementation . . . . .	27
4.1	Microcode Sequences . . . . .	33
4.2	Synthesis results for pPIM architecture with ISA. . . . .	36
4.3	Synthesis results for FPGA implementation of pPIM ISA . . . . .	38
1	List of Publications and Submissions on pPIM Architecture . . . . .	43

# Chapter 1

---

## Introduction

### 1.1 Motivation

Computer architecture is continually pushing to improve their performance where possible. Most of this improvement is focused on the improvement of computer processors which improve at a rate of approximately 60 percent every year. Meanwhile, Dynamic random-access memory (DRAM) architecture is only improving at a rate of 10 percent every year [3]. The large difference in improvements made leads to a growing divide that throttles the overall computer system's performance. Still, the main focus of DRAM architectural design is on reducing sizes and increasing capacities. The differing focus of these two groups continually increases the divide between performance improvement at an exponential rate creating a problem that is commonly referred to as the "memory wall"[4]. The "memory wall" is best defined by a growing divide between processing power and memory bandwidth, depicted in Figure 1.1. This has lead to multiple improvements that remedy the issue brought on by this "memory wall". The memory wall has become so prevalent that the avoidance of it has driven a great deal of research and innovations.

When a miss occurs that requires memory access there are multiple downsides that can occur. The most commonly considered downside is the delay that occurs. In the case that a miss occurs, several communications are required with memory in

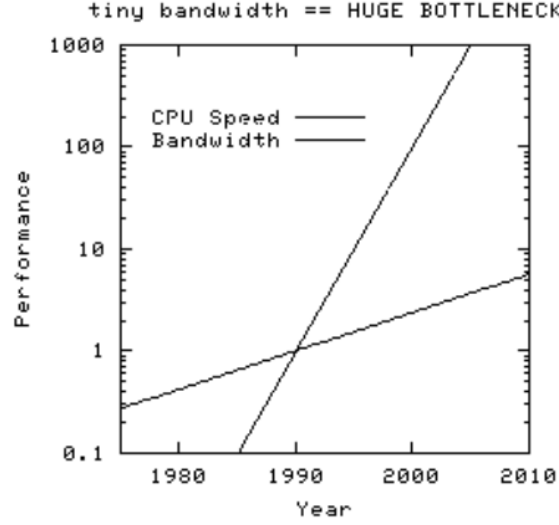


**Figure 1.1:** The growing divide between processor speeds and memory bandwidth that leads to a throttling of processor performance [1]

addition to the desired data. This can lead to delays that could take hundreds of cycles. Each memory access also incurs a large power cost to transfer the data from the DRAM over to the processor. The power required for this data transfer can reach up to 42% [5] of the total power cost. Even if the data is transferred over to the memory before it is accessed, the downside of the power cost for the data transfer is still incurred on the system. Each of these problems become especially burdensome with data-intensive applications such as machine learning models that require large transfers of data to be processed.

While the average consumer might not see heavy impacts of delays from memory accesses, enterprise and research computing frequently collide with the "memory wall". Commercial and scientific computing will often deal with much larger quantities of data that the average consumer which can present itself in various ways. These applications can vary from large databases of user data to datasets and weight information for training machine learning models. This causes commercial and scientific computing to see idle times that average around 65 percent and 95 percent[1].

With the bottleneck of the "memory wall" approaching and increase in data-

intensive applications, architectures that subvert the issue of communication latency and power consumption are increasingly important. Technologies that are capable of performing processing within the memory will be able to subvert these issues by performing bulk operations without the need of transferring the data from the memory to the processor. A reprogrammable processing in memory (PIM) architecture will improve computer systems by providing an adaptable hardware accelerator within memory and reduce idle times spent waiting on data transfers from memory.

# Chapter 2

---

## Background

### 2.1 Processing-in-Memory

PIM is a type of processing architecture that takes a step away from traditional Von Neumann techniques. In Von Neumann architecture there is generally a separation between processing power and the memory architecture. Instead of introducing processing power closer to memory, caches are built into the processor to reduce the number of memory accesses. Large portions of the die are dedicated to the cache, but memory accesses still result in misses. If a large dataset is required and is not present in the cache at processing times, large latencies will occur and reduce the performance. PIM architectures attempt to subvert this problem by introducing processing elements to the memory. Instead, commands can be sent to the PIM architecture to handle the processing so that a large data transfer is not necessary.

There have been various PIM architectures proposed over previous years that focus on different aspects of processing. Certain approaches attempt to avoid introducing new hardware for processing. These architectures instead propose methods that take advantage of existing DRAM architectures by reading multiple rows at once [6, 7]. This is limited in that it is useful only for bitwise operations and that any data must be row-aligned.

Other PIM architectures propose the introduction of new processing elements

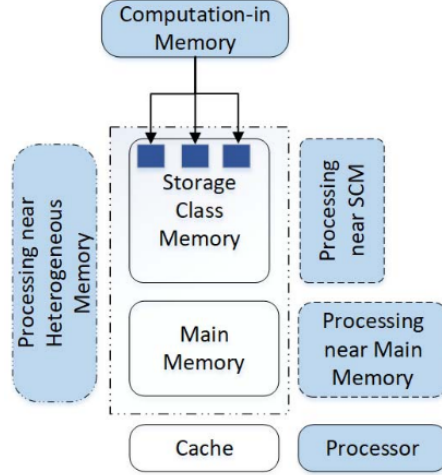


**Figure 2.1:** The various types of processing with respect to their interaction with memory. Traditional architectures include a cache coupled with processors. More recent architectures have attempted to reduce the distance of memory from the processing power to reduce delays with 'near memory' approaches. PIM goes a step beyond and introduces the processing power within the memory architecture for further reduced latencies[2].

into the memory that are focused at improving the performance of specific operations similarly to hardware accelerators. LUT-based Fast and Accurate Vector Multiplication in DRAM-based CNN Accelerator (LAcc) improves upon multiplication speeds through the use of LUT-based multipliers within memory[8]. Another architecture, Latch-up Based Processing In-Memory System (LUPIS), performs operations such as addition and multiplication within non-volatile memory with lower latencies [9]. DRISA and DrAcc both use bit shifters to accelerate the MAC operations of CNN [10, 11]. Some PIM architectures even look into the use of RAM types other than DRAM. The PRIME takes an application specific approach to the problem by accelerating the performance of Neural Networks within resistive random access memory (ReRAM)-based main memory [12].

While these architectures provide an improvement on specific operations of existing computer architectures, they lack the ability to adapt or be reprogrammed for alternative applications. The programmable-PIM (pPIM) architecture is a look-up table (LUT)-based PIM provides greater adaptability [13, 14]. The pPIM avoids re-



stricting the user to accelerating specific functions by allowing the reconfiguration of LUTs with function words. The pPIM architecture has been published previously in Computer Architecture Letters(CAL) and is currently submitted with minor revisions for Transactions on Parallel and Distributed Systems (TPDS).

## 2.2 Instruction Set Architectures

The instruction set architecture (ISA) associated with a hardware is an integral component that bridges the gap between the hardware and the software applications that can be used with the hardware. DUE to the nature of both memory and PIM these ISAs are designed to take instructions from external host processors[15, 16, 17]. Memory is already a passive element that operates off instruction from an external host[18]. Implementation of an ISA with memory will see less difficulty if the ISA also has a passive design. Additionally, PIM architecture is often focused on accelerating big data applications, such as neural networks, which often perform repetitive operations over bulk quantities of data[2, 19]. An ISA for PIM should reflect this focus of the architecture. Instead of executing entire programs the ISA should be focused on accelerating computations required by the host in a single-instruction multiple-data manner. It is also important to design a PIM ISA with a low level of complexity. If the ISA becomes too complex, the ISA could take up large swaths of area or power and become too costly to reasonably include within the DRAM.

Microcode offers a viable solution to the problem of over complexity and area. Microcode is a form of programming that is done at the control signal level. This form of coding is capable of performing operations that otherwise would require the introduction of new hardware. Microcode usage for an ISA is especially useful in the DRAM where a reduction in the hardware will reduce the area that will be taken from the DRAM memory to integrate the component. Instead of using physical space required for hardware components of the ISA, the microcode of a PIM architecture

could be stored into the memory. This also allows for a reprogrammable ISA that can be changed to suit the needs of the host processor.

## 2.3 Neural Networks

Neural networks are abundantly common in machine learning models for their ability to perform classification. These layers appear in varying formats such as dense layers and convolutional neural networks. These variations do have in common that they perform matrix multiplications on datasets that are often large in size. Performing such an operation requires that a multiply accumulate operations be repeated throughout the datasets and the weights of the model.

Other components involved with neural networks in machine learning models include the functions used for classification and activation. Classification of the final output layer can be done by determining the index of max value in the set.

The activation layer of a neural network is used to remove the linear relationship between the input and the output of a neural network layer. If a linear activation layer is used, displayed in Equation 2.3, the output will maintain a linear relationship with the input and not necessarily be the best representation of the relationship between the input and the expected output. Non-linear relationships are used to avoid this problem when training neural networks. Some of the most common activation layers being sigmoid, tanh, and Rectified Linear Unit (ReLU).

$$f(x) = x \tag{2.1}$$

Equation 2.3 depicts the sigmoid activation function that scales an output between 0 and 1. With the range from 0 to 1, the output can be interpreted similar to a probability which is useful in a classification. Due to the high derivative in the center

of the functions, the model is also very useful in training. In backpropagation, the high derivative forces the weights towards the extremes.

$$f(x) = \frac{1}{1 + e^{-x}} \quad (2.2)$$

The tanh is a trigonometrical activation function that improves upon the sigmoid function. Instead of scaling to a range from 0 to 1, the tanh function scales from a range from -1 to 1. This is useful in classifications where the presence of a certain input may lead to strong confidence that a classification should not be made.

The ReLU activation function was introduced due to the high complexity of the sigmoid and tanh activation functions that led to longer training times. ReLU takes the simplicity of the linear unit and introduces a non-linear behavior to the function by rectifying it, or producing an output of 0 for any negative input.

$$f(x) = \max(0, x) \quad (2.3)$$

The ReLU activation is currently one of the most commonly used activation layers in neural networks. The ReLU activation activation, depicted in Equation 2.3, requires very little computation power. Since the only operation it performs is setting negative values to zero, it often leads to quicker training. It also will also often output sparse matrices, which are matrices with a large presence of zeros throughout it.

The tanh function is an activation that is used to scale the outputs of a layer to a value between -1 and 1.

## 2.4 Supporting Work

Introducing a PIM architecture can often be difficult due to the lack of existing architecture that leaves DRAM in a position to under-perform in processing. One reason for this is the lack of existing architecture for efficient data movement among subarrays. It is restricting for a PIM architecture to be limited to only using the data within a single subarray. Even with access to data external to the coupled subarray, data accesses can be costly in terms of power and latency. RowClone tackles this issue by proposing an efficient method for copying bulk data between subarrays at low energy cost [5]. Low-Cost Inter-Linked Subarrays (LISA) further expands on the RowClone architecture by proposing an architecture that is capable of providing fast memory copying between subarrays at low cost to power[20].

Introducing a PIM architecture must also provide a sufficient boost in the performance that provides a benefit to a system. A design that is either slow or has a high power will likely diminish the performance benefits that are produced by reducing the memory transfer between the host and memory. For this reason, LUTs have been frequently used in PIM designs. LUTs have shown that they are capable of producing fast designs at low power costs[11, 10, 8]. The use of LUTs can also provide reconfigurability to a design so that it can be adapted to multiple applications.

## Chapter 3

### pPIM Architecture

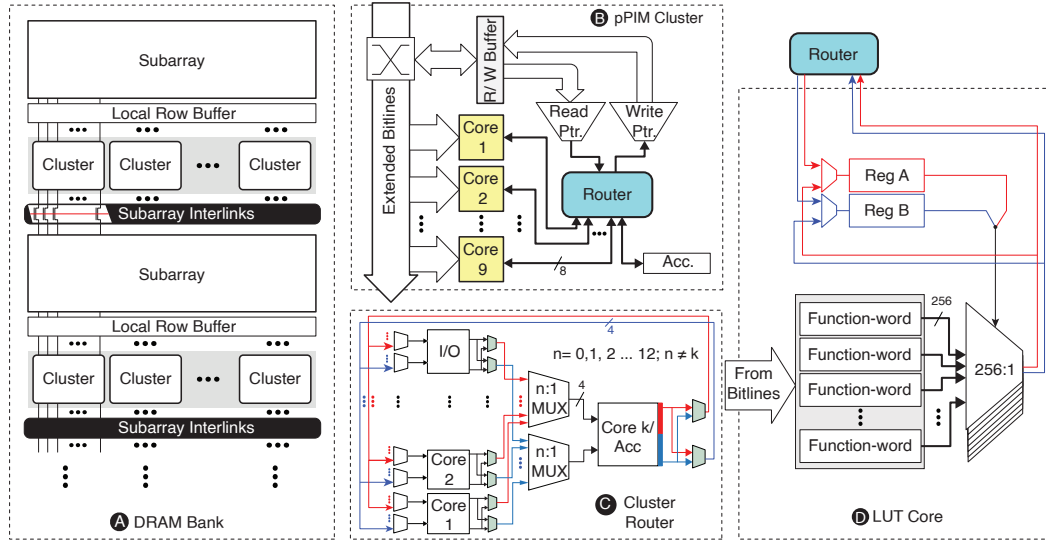


**Figure 3.1:** Heirarchical view of the pPIM architecture

The proposed pPIM architecture's is a PIM architecture design focuses on performing data-intensive applications. The hierarchy of the proposed architecture is depicted in Figure 3.1. An additional goal of the design is to be reprogrammable to fit a wide variety of applicatinos. The design accomplishes this in architecture with a LUT-based design. The pPIM architecture consists of a pPIM cluster at the top level. Within each cluster are multiple pPIM cores that enable reprogrammability within the architecture.

### 3.1 pPIM Core

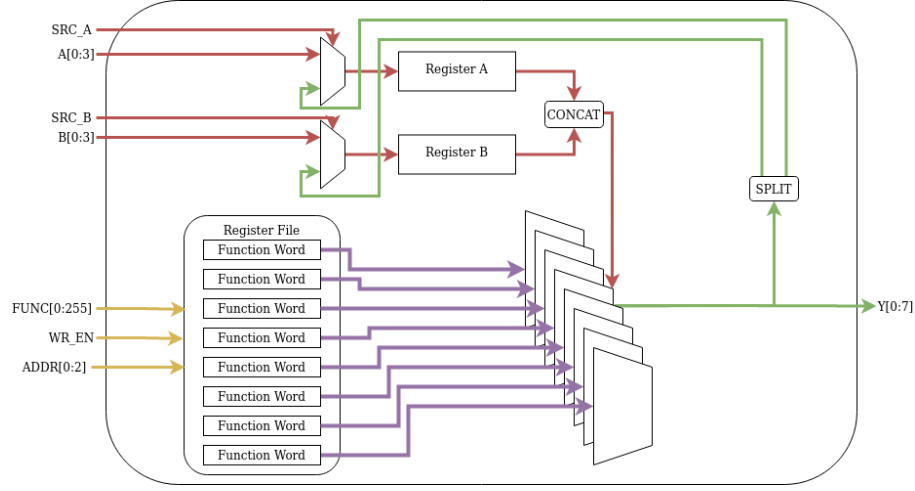


**Figure 3.2:** Layout of the pPIM core architecture.

The base processing element of the pPIM architecture is the pPIM core. The design of the pPIM core is shown in Figure 3.2. The pPIM core is responsible for a majority of the computational power within the pPIM architecture. Processing within the core is handled through the congregation of LUTs into multiplexers. A majority of the reprogrammability is also handled within the pPIM core through the use of a register file that feeds into the LUTs.

Various functions are capable of being represented by the pPIM core. A function that is capable of being programmed into the pPIM core is any function that consists of two 4-bit inputs and a single 8-bit output. The two inputs can also be treated as a high and low segment of the input if a function contains a single operand. This functionality is accomplished by the pPIM core through the use of an array of LUTs that form eight 256-to-11 multiplexers. Input to the multiplexers is determined by the data within the register file of the pPIM core. Conversely, the select lines of the multiplexers are determined by the two input vectors to the pPIM core.

Within the pPIM core's register file are eight function words. Each of the function words are eight bits in length to fit the input to the 256-to-1 multiplexers. Each of

the functions words are then associated with a single bit position within the output of the pPIM core.

### 3.2 pPIM Cluster

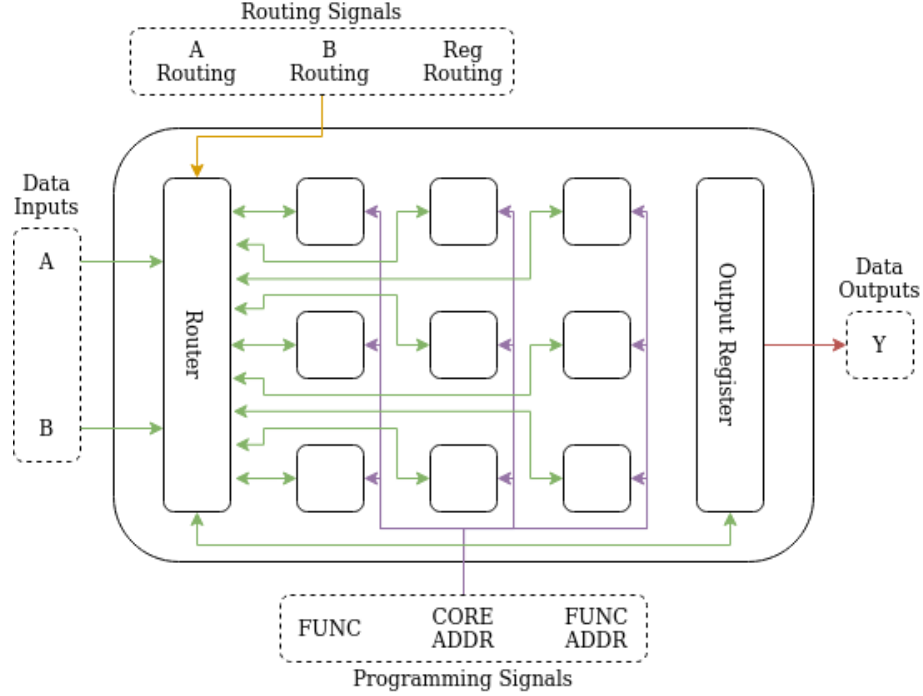


**Figure 3.3:** Layout of the pPIM cluster architecture.

At the top level of the pPIM cluster is the pPIM cluster. The structure of the pPIM cluster is displayed in Figure 3.3. The pPIM cluster combines the use of multiple pPIM cores, interconnected by a router. Combining functionality of multiple pPIM cores allows the pPIM cluster to perform more complex operations over a single or multiple stages. The added functionality includes performing operations that require greater resolution than the inputs and operations that require more than two operands.

Each pPIM cluster contains nine pPIM cores that provide computational power. The pPIM cores within a pPIM cluster are individually programmed, maximizing the flexibility of the design to adapt to various applications. The dataflow within the pPIM cluster requires an all-to-all communication network with minimal

overhead. This is accomplished through the use of a crossbar switch architecture. Through the use of a crossbar switch routing architecture, each pPIM core can receive input from the outputs of any other pPIM core within the pPIM cluster. To match the size of the inputs and outputs of the pPIM cores within the routing architecture, the 8-bit outputs are treated as two 4-bit segments.

### **3.3 pPIM Function Word Generation**

Adaptation of a pPIM core to perform a specific function requires the generation of eight function words. This requires determining the output of the pPIM core for each possible input pairing. The process must pass over 256 possible input pairings to determine an entire function words. During each iteration, the bits of the output are split up and set in their respective function words at the index of the current iteration. While not all functions can be fully realized on the pPIM core due to the resolution, additional steps can be taken for approximation on the architecture. For approximation, an output can be quantized so that it is represented by an 8-bit output format.

### **3.4 pPIM MAC Operations**

As a demonstration of the capability of the pPIM to be used in data-intensive operations, functionality for MAC operations is mapped onto the architecture. Flexibility is additionally demonstrated through mapping MAC operations for multiple data types and precisions. MAC operations for both unsigned and signed integers at 8-bit and 4-bit precision dataflows are generated.

Performing a MAC operation with inputs restricted to 4-bits requires the calculation of the result through partial products. The calculation of a multiplication through partial products is outlined in Figure 3.4. This requires multiplying 4-bit



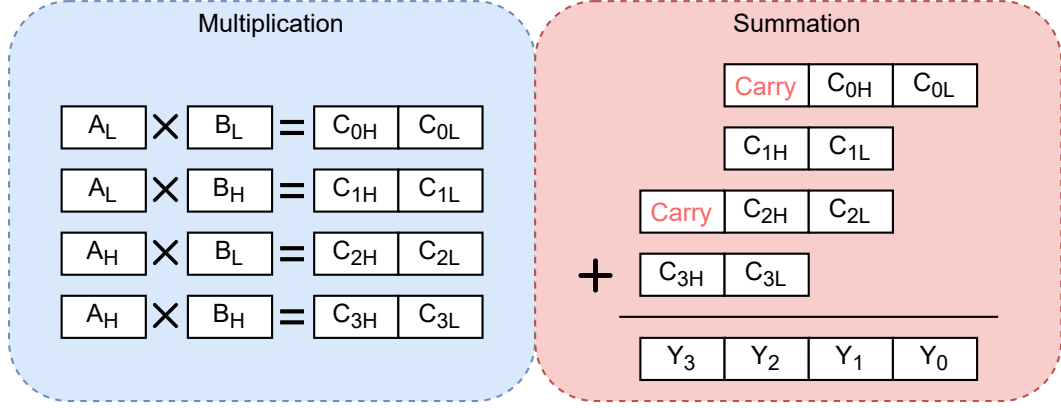


**Figure 3.4:** Calculation of the result of an unsigned multiplication through the calculation and summation of partial products.

segments of the operands to generate partial products. Each of the partial products are then summed together to determine the value of the result. The resulting segments are then accumulated into the value of the accumulator to perform the MAC operation.

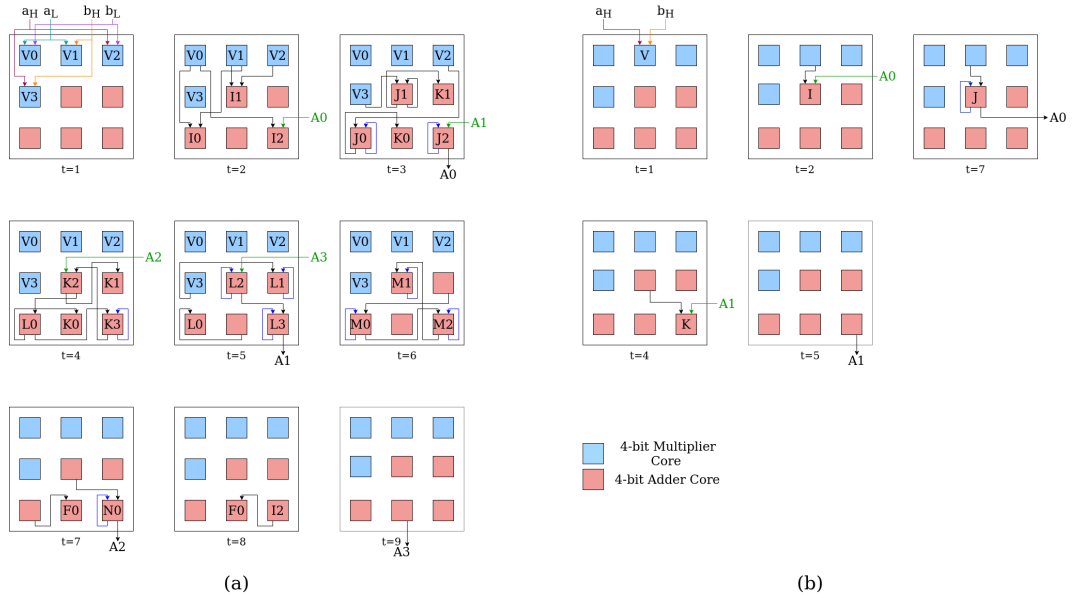


**Figure 3.5:** Model of dataflow within a pPIM cluster for both (a) 8-bit full precision and (b) 4-bit half precision unsigned MAC operations

When mapping the MAC operation to the pPIM architecture, each individual computation with a segment can be associated with an single computation on a pPIM core. This produces the dataflow for both 8-bit and 4-bit precisions displayed

in Figure 3.5.

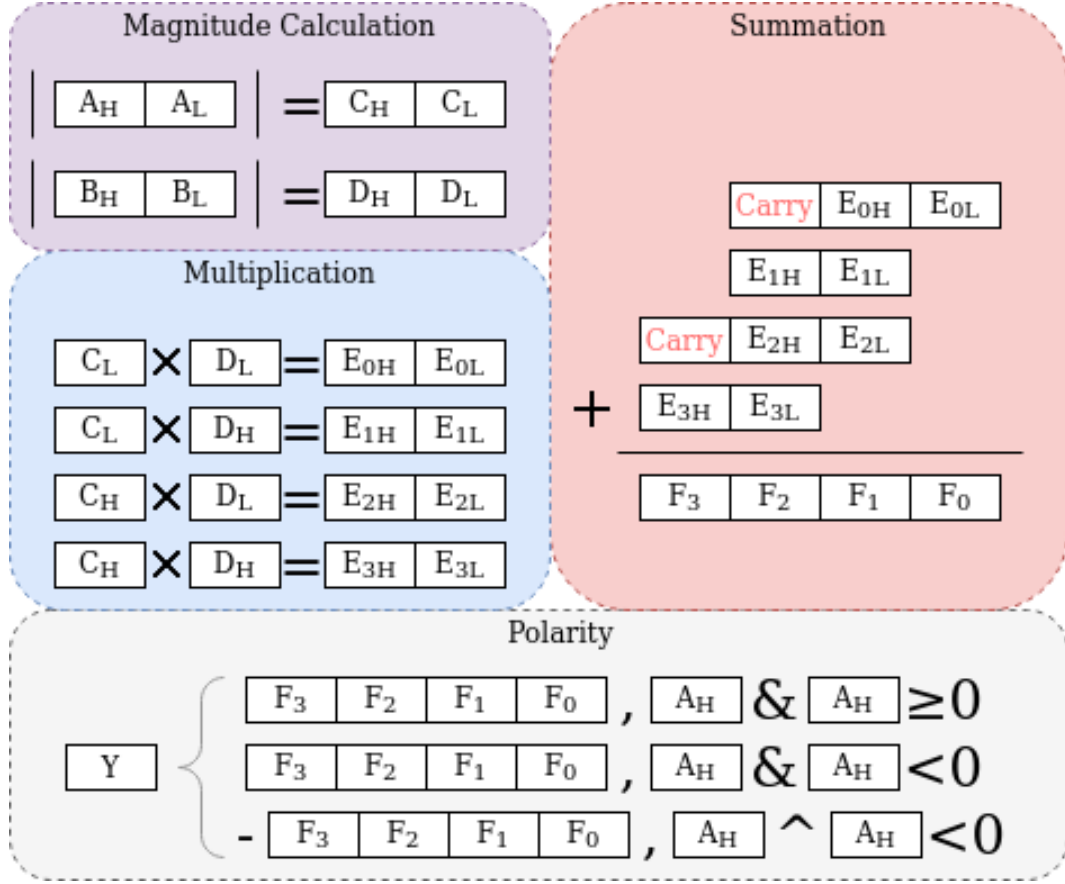


**Figure 3.6:** Calculation of the result of a signed multiplication through the calculation and summation of partial products.

Calculating the result of a signed MAC operation requires additional steps to handle the polarity of the integer. This is due to differences in the multiplication of signed and unsigned integers. Handling the multiplication for the signed integers is done by first finding the magnitude of each operand. The magnitude of each operand can be handled with the unsigned multiplication configuration. Summation is handled the same with both the signed and unsigned numbers. Once the summation of the partial products is completed, the polarity of the integer is determined based off of the polarity of the operands. Figure 3.6 outlines the process taken to reach the final product of the multiplication. The result is then accumulated with into the accumulator.

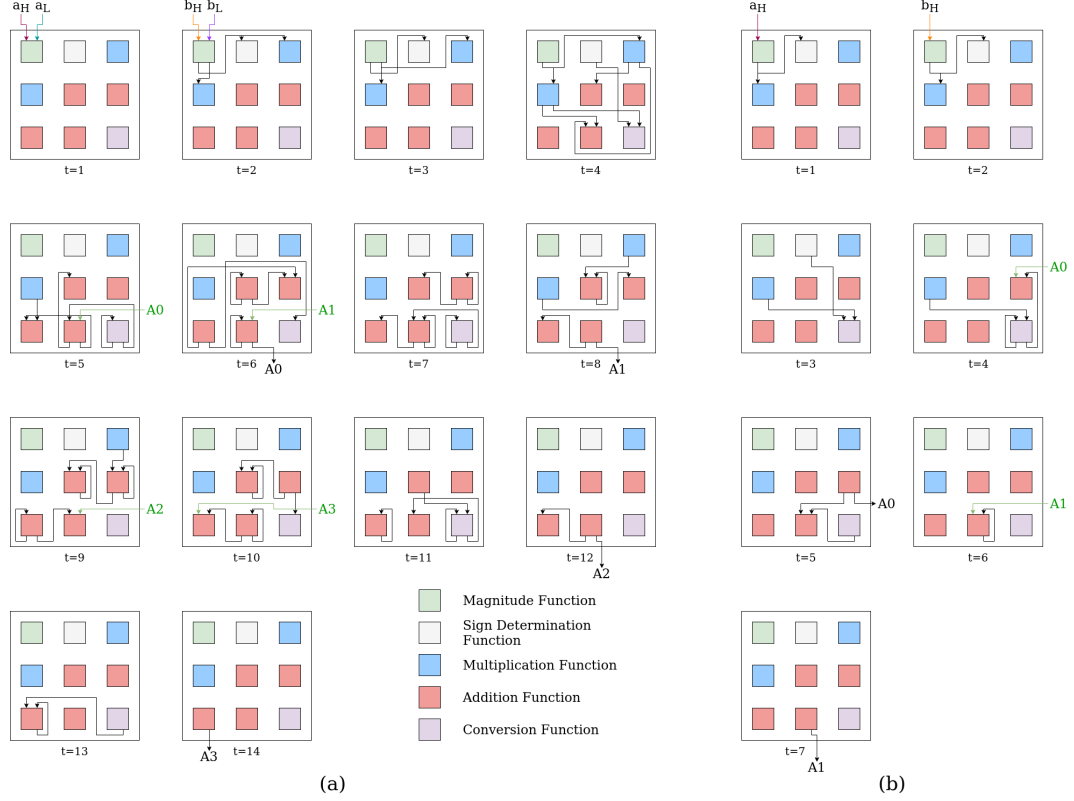


**Figure 3.7:** Model of dataflow within a pPIM cluster for both (a) 8-bit full precision and (b) 4-bit half precision signed MAC operations

Similarly to the unsigned integer MAC dataflow, the signed integer MAC dataflow can be constructed from the partial products calculation. Figure 3.7 displays the dataflow for a signed MAC operation with both 8-bit and 4-bit precision.

### 3.5 pPIM Activation Operations

Versatility of the pPIM architecture to adapt to represent multiple operations was demonstrated through the mapping of several common activation operations used with CNNs. The mapped operations include ReLU, Linear, sigmoid and tanh.

Performing the ReLU activation operation only requires a single pPIM core. Figure 3.8 depicts the dataflow for the ReLU activation. Output of the ReLU operation is only set to zero if the input is negative. Due to this, the highest segment is used for determining the output at each segment.

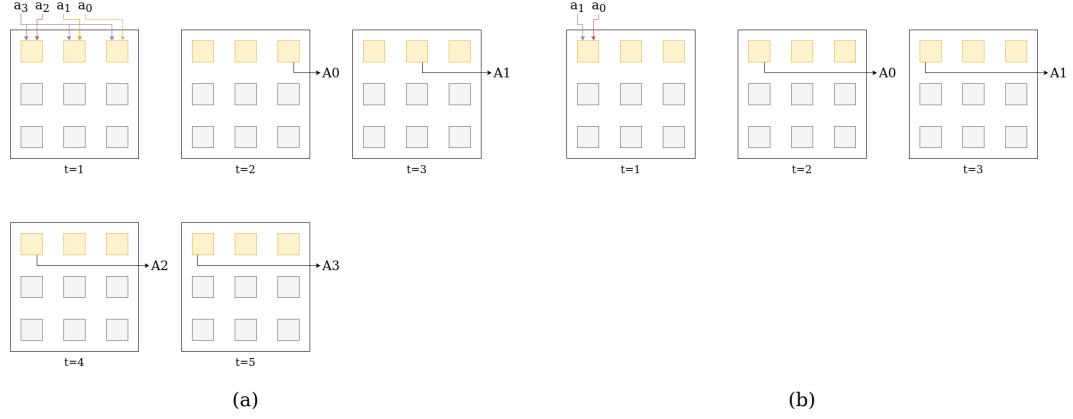


**Figure 3.8:** Model of dataflow within a pPIM cluster for both (a) 16-bit precision and (b) 8-bit precision ReLu activation operations.

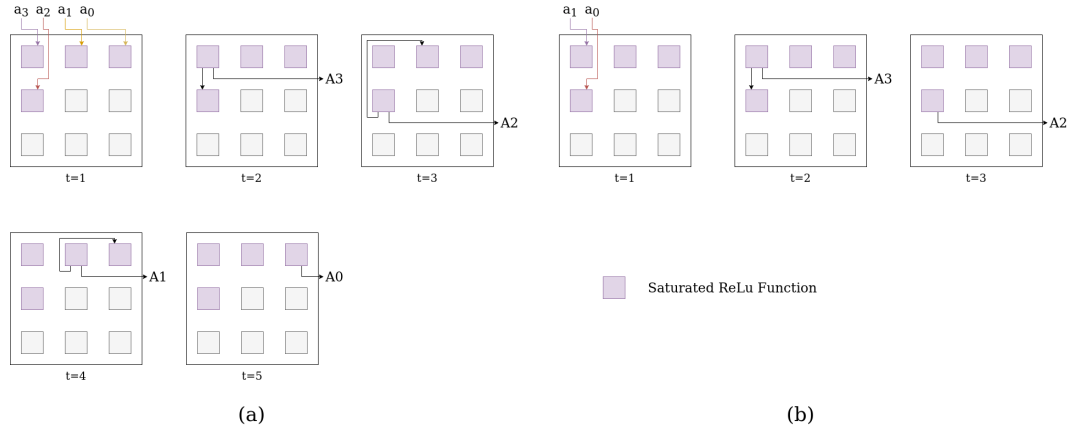


**Figure 3.9:** Model of dataflow within a pPIM cluster for both (a) 16-bit precision and (b) 8-bit precision saturated ReLu activation operations.

Saturated ReLu activation has added complexity to the configuration. Each segment will have an associated value with the maximum. However, the segment will not be set to the max value if one of the segments at a higher position did not reach its maximum value. The dataflow for the saturated ReLu activation is displayed in Figure 3.9.

Sigmoid and tanh are capable of being approximated on the pPIM architecture. A single pPIM core can approximate either an 8-bit sigmoid or 8-bit tanh in a single cycle. Scaling can also be done based on whether the input is a fixed point value and the placement of the decimal within the input.

Due to the lower complexity of activation operations within a pPIM cluster, mul-

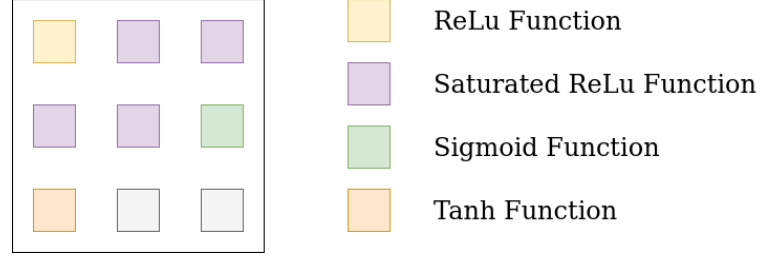


**Figure 3.10:** Configuration of a pPIM cluster for quick switching between activation operations.

multiple activation operations are capable of being configured into a single pPIM cluster. This eliminates the process of reprogramming a cluster to perform a different activation operation. Figure 3.10 displays a pPIM cluster configured to perform ReLu, saturated ReLu, sigmoid, and tanh activation operations.

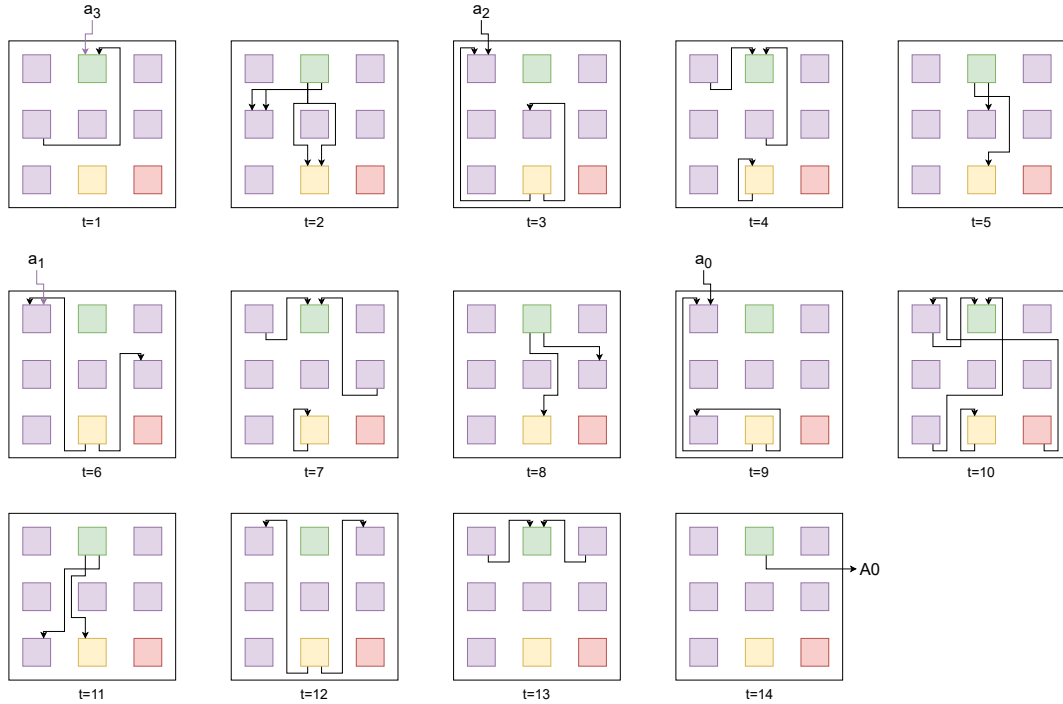


**Figure 3.11:** Model of dataflow within a pPIM cluster for a 16-bit max-index operation.

Additionally, the index of a classification is capable of being determined in the pPIM cluster. The dataflow for this max-index operation is displayed in Figure 3.11. The configuration consists of several pass cores, a comparison core, a conditional core, and a counter core. Since only a single 4-bit segment of a cluster is capable of

being compared at a time, each segment needs to be compared individually. These comparisons begin with highest priority given to the most significant segment. If one segment is greater than the other, the conditional core will prevent the input from passing its value on to the following stages. Otherwise if the segments are equal, the values will pass on and continue to be compared. In the final stage, the value of the counter is passed on to the comparison core if the current operand is the new max value. The comparison will then update the accumulator stored index if the index is passed and vice versa.

### **3.6 FPGA Implementation**

An FPGA implementation of the pPIM architecture is proposed for the validation. Focus of the implementation is on validating the processing elements and dataflow through the simulation of unsigned 8-bit MAC operations on multiple pPIM clusters. Classification is also handled by a pPIM cluster with a max-index dataflow. The final implementation is used to predict numbers within images with a single layer NN.

#### **3.6.1 Technology & Resources**

Implementation of the pPIM architecture is run on the ZC702 base board. The ZC702 base board delivers a package with both a programmable logic (PL) core and processing system (PS). Implementation of the pPIM clusters is done solely on the PL in a hardware descriptive language. Other features, such as communication with the architecture are handled on the PS.

The dataset chosen for training and testing of the NN is the Modified Standards and Technology (MNIST) dataset. Examples of images from the MNIST dataset are displayed in Figure ???. Within the dataset is a compilation of 70,000 images of handwritten digits, split into a training set of 60,000 images and testing set of 10,000 images. Images in the MNIST dataset are standardized to be in grayscale

with dimensions of 28 pixels by 28 pixels.

Training of the NN is handled on Tensorflow before exporting into the FPGA implementation. Tensorflow also provides access to the MNIST dataset for training the model external to the ZC702 base board and testing the model on the board.

### **3.6.2 Machine Learning Model**

The model trained for the validation of the pPIM architecture is a single layer NN. The NN accepts input in the format of an input vector of 784 pixels, each with an 8-bit unsigned integer value. The output of the model is a single numerical prediction for the digit in the image, ranging from zero to nine.

The single NN layer within the model is a fully connected layer with no biases. The output of the layer is a vector of ten 8-bit unsigned integers, the index of which is relative to the digit that its prediction is associated with. The size of the weight vector to handle an input with a size of 784 and output size of ten is a matrix with the dimensions 10x784. Classification of the output vector is done with a max-index operation where the index of the highest value prediction is the classification made on the image.

### **3.6.3 pPIM Implementation**

The FPGA implementation of the pPIM architecture is divided into two separate regions: MAC operations and max-index operations. The FPGA implementation of the two regions is depicted in Figure 3.12. A separate region is allocated to the two operation types within the FPGA and neither is reconfigured. This is due to the focus of the implementation on validating the way in which the pPIM architecture processes data. Instead of requiring additional steps to handle the programming of each cluster, constants are set into the pPIM cores' register files.

To handle the dataflow and execution, each of the regions is coupled with a finite

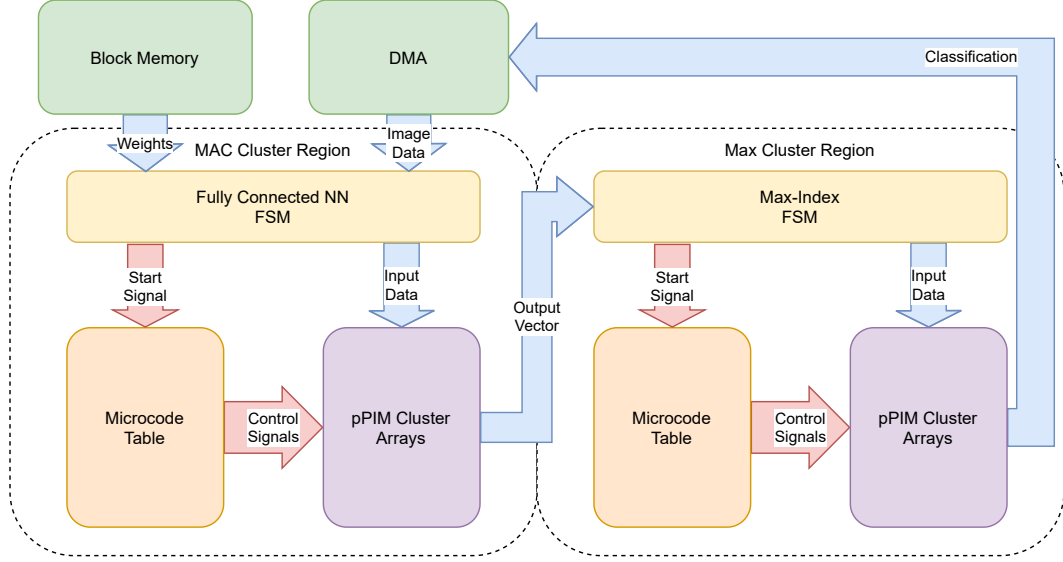


**Figure 3.12:** Structure of the multiple region approach to designing an FPGA implementation of the pPIM architecture.

state machine. The The state machine is responsible for tracking input and output to the region and beginning execution. When each cluster has its input ready, the state machine sends a start signal to begin the execution. Once each of the inputs have been processed, the state machine also sends the output to the next region or memory.

### 3.6.4 Communication

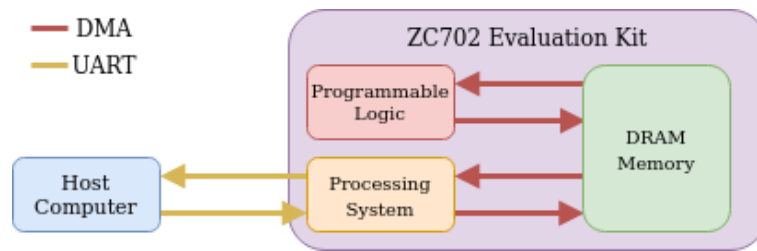


**Figure 3.13:** Communication model between multiple elements within the ZC702 evaluation board and the host CPU.

Communication between the host computer and elements on the ZC702 base board required the use of two communication protocols: direct memory access (DMA) and universal asynchronous receiver-transmitter. The communication used between each



of the elements in the implementation is shown in Figure 3.13.

The PS on the board provides hardware for UART communication. Over the UART communication, the external host CPU is capable of communicating with the PS. Over the UART communication the image data is passed from the host CPU to the PS. The PS is also responsible for sending the image classification back to the host CPU.

Both the PS and PL on the board are capable of DMA. DMA on the PL requires introducing IP provided by Xilinx that communicates the data to the pPIM architecture over an advanced extensible interface (AXI). Communication over DMA is used to transfer the image data to the pPIM architecture and for the pPIM architecture to return a classification on the image.

## 3.7 Results

### 3.7.1 pPIM Characteristics

**Table 3.1:** Synthesis results for pPIM architecture.

Component	Delay (ns)	Power (mW)	Active Area $\mu\text{m}^2$
pPIM Core	0.8	2.7	4616.85
pPIM Cluster (MAC Operation)	7.2	5.2	41551.66

The pPIM architecture is modelled in post-synthesis using the Synopsys Design Compiler at a technology node of 28nm. Characteristics from the post-synthesis model are recorded in Table 3.1. The model includes both a synthesized model of the pPIM core and the pPIM cluster. Synthesis of the LUT multiplexers is modelled using transmission gates, improving the area overhead of the design.

Gaining an accurate estimate of the activity of the pPIM cluster during operation required having an example of the processing performed. An 8-bit unsigned MAC

operation is chosen to record the power and delay figures for the pPIM cluster. This gives an accurate estimation for analysis on deep learning models that contain MAC operations for a majority of operations.

### 3.7.2 Performance Evaluation

The performance of the pPIM architecture is evaluated in a comparison against various computational architectures. Architectures include contemporary PIM architectures DRISA and LAcc, as well as high-performance computing architectures Intel Knights Landing CPU (KNL) and Nvidia Tesla P100, and AI accelerators Edge TPU. For an accurate comparison of each architecture, each architecture is analyzed at 28nm performance. The comparison takes a look at the performance of each of the architectures in various popular deep learning models. These models include Alexnet, Resnet 18, Resnet 34, Resnet 50, and VGG16. Evaluation of the pPIM architecture on each CNN is performed through analysis of how quickly the synthesized model can perform the computation in the CNN. The results of the analysis of each architectures throughput, energy, and area is displayed in Figure 3.14, 3.15, and 3.16, respectively.

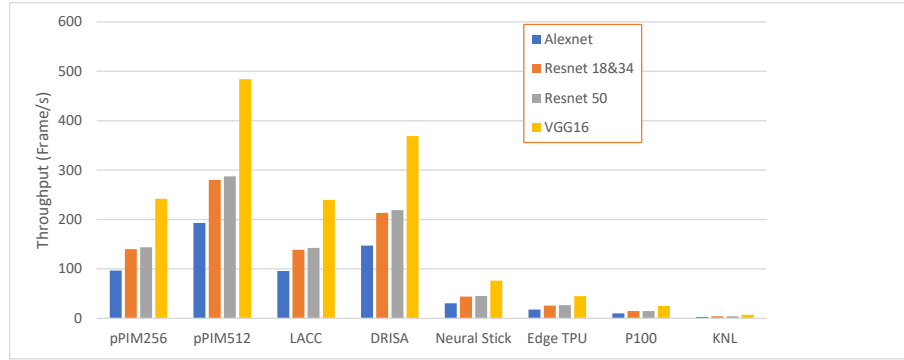


**Figure 3.14:** Comparison of various high-performance architectures on their throughput with popular deep learning models.

A noticeable gap between exists in the results between the throughput of the PIM architectures and the traditional architectures. The difference in performance can be attributed to the delays incurred by accessing memory. Despite being designed to

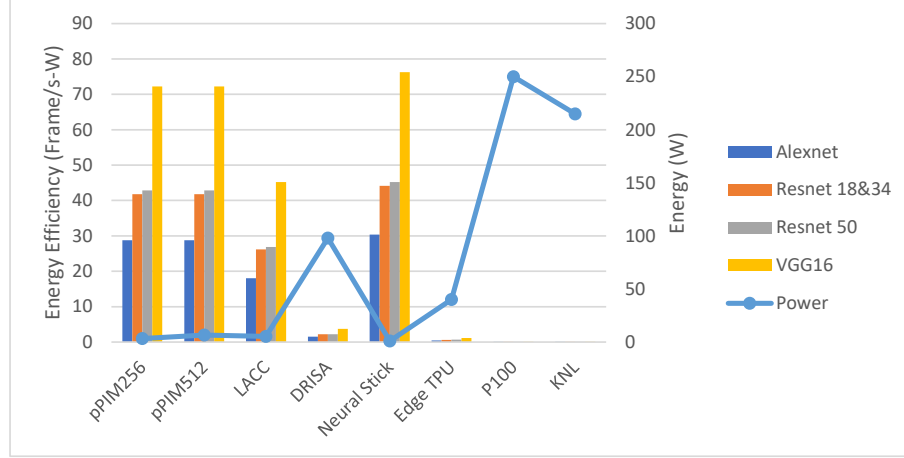


**Figure 3.15:** Layout of the pPIM cluster architecture.

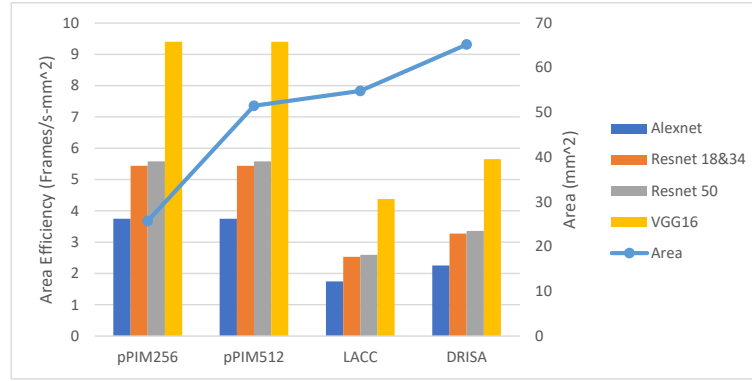


**Figure 3.16:** Layout of the pPIM cluster architecture.

have high-performance, these architectures still run into the limitation of memory access. Many of these architecture also have low energy efficiency as they require larger systems to be introduced into the computer system. This is unlike PIM architectures which are introduced to existing memory architecture, keeping their energy efficiencies higher. Even architectures such as the neural stick that deliver a high energy efficiency have this benefit outweighed by its non-competitive throughput with the PIM architectures.

Among the PIM architectures, the two highest throughputs were seen with in the pPIM 512 cluster configuration and DRISA. The DRISA architecture, however, is not an efficient architecture. DRISA parallelizes operation throughout multiple memory banks. This increases both the area overhead and power consumption, leading DRISA

to have the largest area and energy usage among each of the PIM architectures. The pPIM 512 cluster configuration is able to provide a high throughput while maintaining the highest area and energy efficiency among the PIM architectures, along with the pPIM 256 cluster configuration. Even with a lower throughput than that of DRISA, the pPIM 256 cluster configuration is able to outperform DRISA in terms of its efficiency. LAcc is slightly more competitive in terms of efficiency than DRISA. Despite this, the pPIM architectures outperform LAcc in all areas. This can be attributed to the storage of LUT data within the memory bank, increasing both the area and power costs.

### 3.7.3 FPGA Characteristics

**Table 3.2:** Synthesis results for FPGA implementation

Component	Power (W)
Clocks	0.026
Signals	0.011
Logic	0.011
BRAM	0.016
InputsOutputs	0.001
PS7	1.566

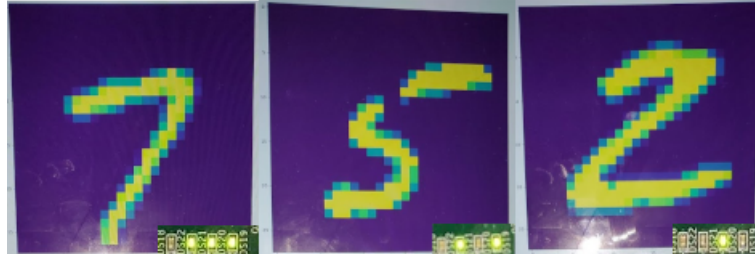
The pPIM architecture is characterized in a post-implementation model using the Vivado Integrated Design Environment. The final model is capable of operating the pPIM architecture at a maximum clock speed of 200MHz. From the post-implementation model, power statistics are gathered from the system. The division of power among the elements on the board is listed in Table 3.2. Approximately 0.065W of the power is consumed by the pPIM architecture within the implementation. The remaining 1.566W are consumed by the PS in transferring the data between the data from the host CPU to memory, where it can be accessed by the pPIM architecture.

## 3.7.4 FPGA Performance Evaluation

**Table 3.3:** Timing results for FPGA implementation

Component	Throughput (Frame/s)
pPIM Architecture	255,102
UART (115200 Baud/s)	14.7

Performance of the FPGA implementation of the pPIM architecture is evaluated for the single layer neural network. The maximum throughputs of both the UART and the pPIM architecture are recorded in Table 3.3. The results display that the performance of the pPIM architecture is high. As expected with data communications across long distances, the UART throttles the maximum throughput of the implementation. There are also added delays in the PS that further throttled the performance of the architecture.

**Figure 3.17:** Predictions made by the pPIM architecture running on the ZC702 base board.

Several images from the MNIST dataset are also sent through the board for classification. The device added use of LEDs to output predictions in the form of a binary value. Several images of predictions made by the pPIM architecture are displayed in Figure 3.17.



## 4.1 ISA Communication

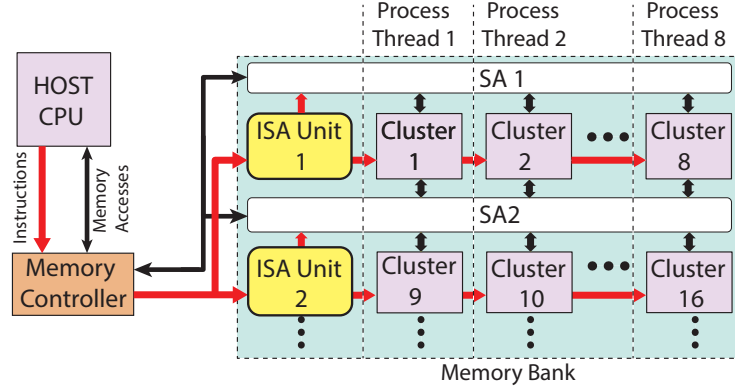


**Figure 4.2:** Model of interface between the ISA with pPIM Clusters and memory elements.

The ISA is in communication with several elements internal and external to the memory. These elements are the pPIM clusters, memory controller, memory subarray, and the host CPU. This communication is outlined by Figure 4.2.

An ISA can control up to eight pPIM clusters within a 'column' in unison. Any action that the ISA performs on a pPIM cluster is also performed on the other pPIM clusters within the pPIM column. This allows the ISA to operate with a higher degree of parallelism while also limiting the overhead introduced into the pPIM architecture.

Communication between the host CPU and the ISA is limited to instructions sent through the memory controller. There is no transfer of data from the ISA back to the host CPU as this is already accomplished by the memory controller. Adding data transfer between the ISA and host CPU would only add unnecessary complexity to the design.

## 4.2 pPIM Microcode

The ISA handles the large number of control signals within the pPIM cluster through the use of micro-coded control words. The micro-coded control words add to the reprogrammability of the pPIM architecture by avoiding operation specific hardware

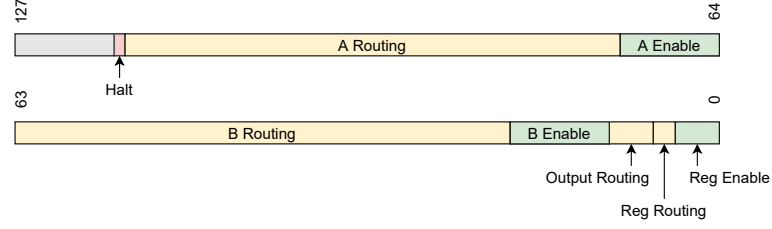


**Figure 4.3: ISA**

to determine control signals. Control words can easily be programmed into the microcode memory to suit a specific operation.

The microcode used by the pPIM architecture is stored into an SRAM memory table, referred to as the microcode table. Within the microcode table is a 2-D array of micro-coded control words that determine control signals sent to a pPIM column for a single cycle. Within the memory, each of the control words are grouped into a microcode sequence. This is a grouping of control words for a single operation ordered sequentially in order of execution.

Each micro-coded control word has a fixed length of 120-bits. The format of the micro-coded control word is shown in Figure 4.3. The control word consists of 119-bits that are dedicated to various signals responsible for dataflow within the pPIM cluster. These signals consist of routing signals, core register enable signals, and output register enable signals. Additionally a single bit is dedicated to communicating the progress of a microcode sequence back to the ISA, referred to as the 'halt' bit. The 'halt' bit is essential to stringing multiple control words into multi-cycle microcode sequences. When high, the 'halt' bit is signaling that a microcode sequence is on the last stage of execution. Conversely, a low 'halt' bit signals that a microcode sequence is currently in execution. This behavior also allows the ISA to know when execution of the next microcode sequence can begin.

Within the microcode table, a program counter is dedicated to stepping through a microcode sequence. When inactive, the program counter points to the first location in memory which contains the control word for an 'idle state'. The program counter



continues to point at this 'idle state' control word until directed to a microcode sequence by the ISA. Once directed to the address of a microcode sequence the program counter iterates through each stage sequentially, cycle-by-cycle. This process continues until the program counter reaches a control word with a high 'halt' bit. The 'halt' bit results in the program counter returning to the 'idle state' to await the ISA to point to the next microcode sequence.

### 4.3 pPIM Instruction Formatting

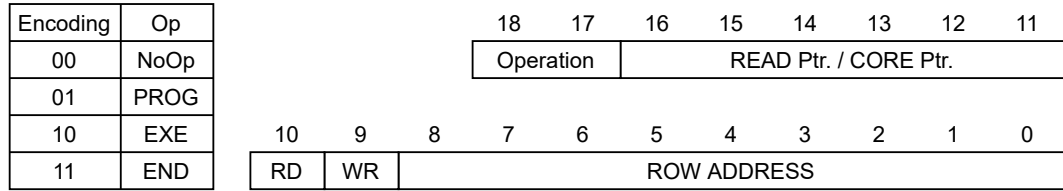


**Figure 4.4:** Formatting of instruction sent from host CPU to pPIM ISA.

Instructions executed by the ISA are formatted in a fixed length of 19-bits. The formatting for the instructions is displayed in Figure 4.4. The instruction format contains two segments dedicated to distinct functions: i) the upper 8-bit segment reserved for handling processing and programming functionality in the pPIM column and ii) the lower 11-bit segment dedicated to memory accesses between the sub-array and pPIM column.

The 8-bit segment of the instruction responsible for the pPIM functionality consists of a 2-bit operation field and a 6-bit pointer field that can address either memory or the register file of pPIM cores. The operation field of the instruction specifies one of three possible operations for the ISA to handle: i) 'PROG', ii) 'EXE', and iii) 'END'. When the 'PROG' operation is specified by an instruction, the ISA begins programming the register file within a pPIM core of each pPIM cluster within the pPIM column. The pPIM core that is begin programmed during the 'PROG' operation is specified by the lower four bits of the 6-bit pointer. When an 'EXE' operation

is specified, the ISA begins execution of microcode sequence within the pPIM column. The starting address of the microcode sequence to be executed is specified by the 6-bit pointer. At the end of a stream of executions, the 'END' operation is sent to the ISA. When the 'END' operation is received, the ISA resets the core. This process includes dumping the output registers of each pPIM cluster to the write buffers, followed by resetting each of the registers. Doing so prepares the pPIM column to receive another stream of instructions. An additional 'NoOp' option is available for selection in the operation field that performs no operation. This is used when only a memory access necessary.

The 11-bit segment of the instruction dedicated to memory accesses between the pPIM clusters and the sub-array consists of a write bit, read bit, and 9-bit row address pointer. The 9-bit pointer gives the ISA the capability of addressing up to 512 memory rows within the sub-array. When the read bit is set high, starting at the specified row address, a byte for each of the pPIM clusters will be written from memory into the read buffers for use in processing. Conversely, if the write bit is set high each cluster will write their output register into the write buffers to be written sequentially into the sub-array at the pointer address. If the write buffers are empty when a request is made, the ISA will force the pPIM clusters to dump their output register data into the write buffer without resetting the clusters. In the event that both the write and read bit are set high, each memory access request is handled individually. First, the ISA will handle the read request. Once the data is stored into the read buffers, the ISA will proceed to handle the write request.

#### **4.4 pPIM ISA Operation Mapping**

The proposed ISA is capable of instructing a pPIM column to perform any pPIM compatible operation. As a demonstration of the process of mapping an instruction to the ISA, the unsigned 8-bit MAC dataflow from Figure 3.5a is mapped onto the

**Table 4.1:** Microcode Sequences

Operation	Stage	Control Word
MAC	1	00 00 00 11 8C 20 0F 00 00 00 4E 53 90 3C 00
	2	00 00 80 60 00 01 50 80 04 02 80 00 05 42 20
	3	30 D2 24 C0 00 01 F0 88 30 0C 00 00 05 42 21
	4	18 00 02 00 00 01 10 C3 50 97 80 00 07 C2 30
	5	30 06 1F 00 00 01 70 40 1D 88 80 00 04 C2 32
	6	18 0C 01 E0 00 01 50 C0 14 0C 00 00 05 42 00
	7	30 C0 00 00 00 01 80 40 00 00 00 00 04 02 04
	8	00 00 00 00 00 00 00 00 03 80 00 00 00 02 01 C0
	9	80 00 00 00 00 00 00 00 00 00 00 00 00 01 C8

ISA.

The process of mapping an operation onto the ISA begins with generation of the microcode sequence from the dataflow. At each stage, each of the control signals are captured to form a micro-coded control word. This sequence is then stored into the SRAM memory that makes up the microcode table. Once stored into the microcode table, the ISA is capable of executing the microcode sequence through an 'EXE' operation. The microcode required to perform a MAC operation is recorded in Table 4.1.

Each pPIM core configuration will also need to be quantified into function words. For an unsigned MAC operation, both multiplication and addition function words are required. These function words are stored into the sub-array to be accessed during the programming step.

Before the MAC operation is ready to be run, each pPIM core needs to be programmed with function words. By running a 'PROG' operation with a read memory request, a single pPIM core has its function words written. This process needs to be repeated for each pPIM core within the pPIM cluster.

Performing a MAC operation on the ISA requires a series of instructions from the host CPU. An example stream of instructions is depicted in the timing diagram in Figure 4.6. The first of the instructions is a read request from memory. This

### MAC Operation Timing

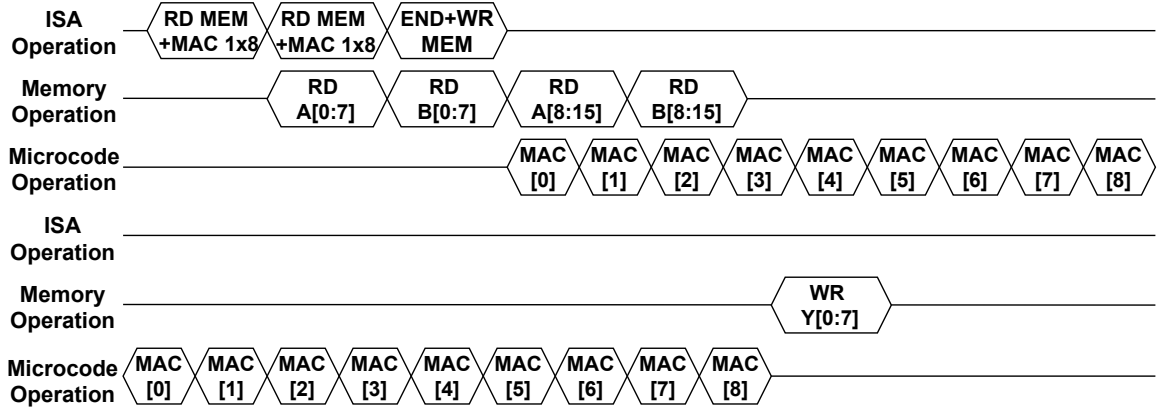


**Figure 4.5:** Timing example of two consecutive MAC operations performed on a pPIM cluster by the pPIM ISA.

reads the operands for the MAC operation into the read buffers of each pPIM cluster. Once the data becomes available to the pPIM column, an 'EXE' instruction with the starting address of the MAC operation is sent to the ISA. The process of reading memory and executing MAC operations can be repeated as many times as needed to accumulate over multiple calculations. Once execution of the MAC operations complete, an 'END' operation stores the output into the write buffers and resets the pPIM column. Output is then stored into memory with a write request to memory.

## 4.5 FPGA Implementation

The FPGA implementation described in Section 3.6 is further developed on an implementation that accepts instructions in the format outlined in Section 4.3. Implementation of the pPIM ISA is used to demonstrate the ability of the ISA to perform MAC operations.

### 4.5.1 Technology & Resources

Implementation of the pPIM ISA is run on the Pynq-Z1 board. The board delivers a package from the same family as the ZC702 board. Additionally, the board had

several PMOD ports available. This allowed the use of a PMOD compatible UART component for communication with the board. The PL is then capable of direct communication with the computer without the need for the UART and DMA of the PS.

### 4.5.2 ISA Implementation

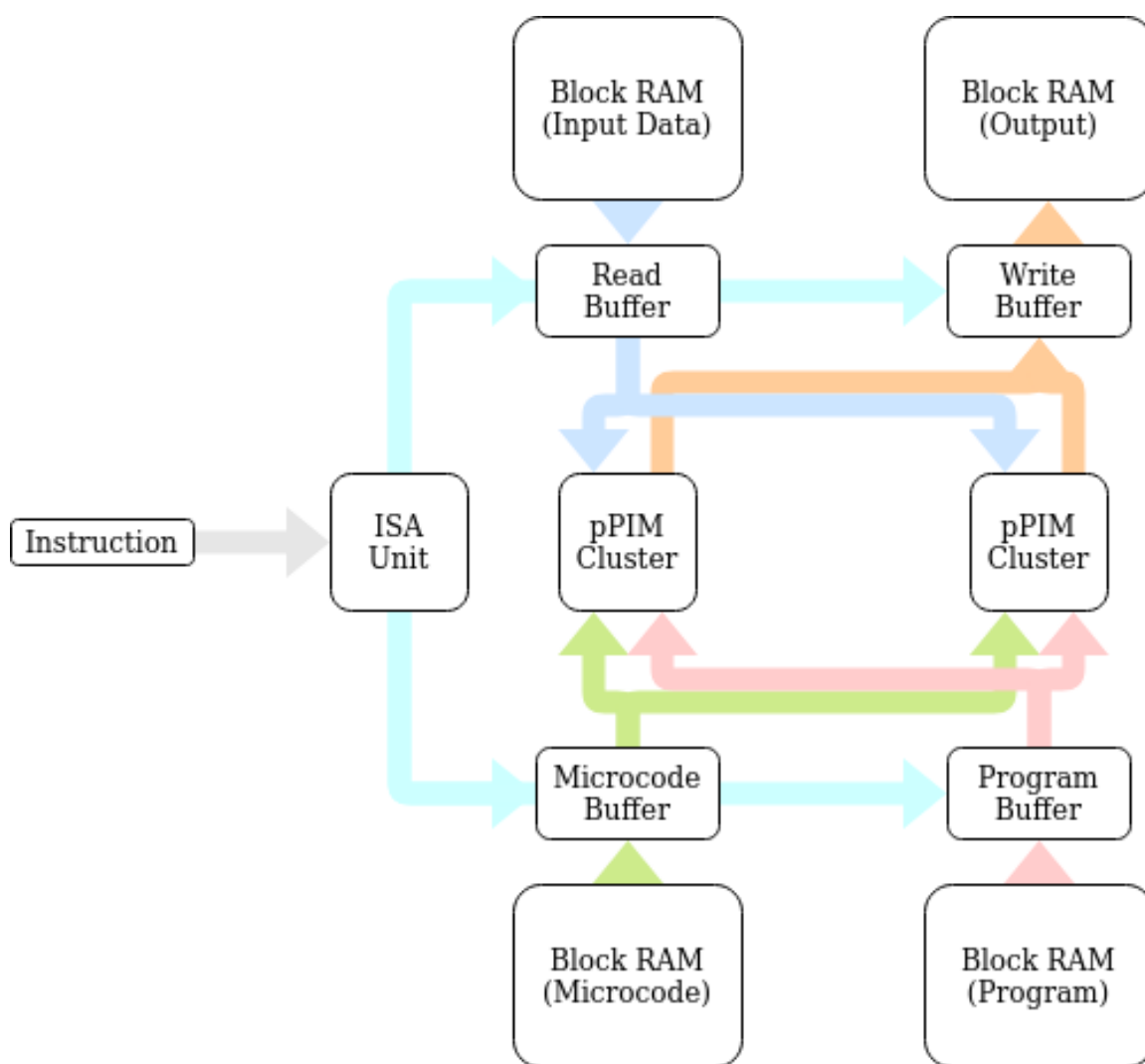


**Figure 4.6:** Timing example of two consecutive MAC operations performed on a pPIM cluster by the pPIM ISA.

The FPGA implementation of the ISA consists of a pPIM column with an ISA unit, 4 pPIM cluster, and buffers to feed data from block RAM (BRAM) into the

pPIM clusters. The structure of the FPGA implementation is outlined in Figure ??.

The implementation demonstrates all of the capabilities delivered by both the pPIM architecture and the ISA. This includes executing microcode, programming the pPIM cores, and making memory accesses.

Each BRAM element in the FPGA implementation is attached to the pPIM architecture with a buffer element. In the design these buffers are responsible for both passing data to the pPIM clusters and communicating control information with the ISA. Control information includes addresses, requests for memory accesses, and whether the buffer is actively performing a memory access.

## 4.6 Results

### 4.6.1 ISA Characteristics

**Table 4.2:** Synthesis results for pPIM architecture with ISA.

Component	Delay (ns)	Power (mW)	Active Area $\mu\text{m}^2$
PIM ISA	0.549	0.155	968.16
PIM Column (MAC Operation)	7.2	43.355	333381.44

The proposed ISA is characterized with a post-synthesis model using the Synopsys Design Compiler at 28nm to match the process used to characterize the pPIM architecture. The resulting characteristics produced by the post-synthesis model are recorded in Table 4.2. The characterization creates a model of both the ISA individually and combines the ISA results with the pPIM clusters to characterize the pPIM column.

Due to the ability of the ISA to parallelize operations within a column and perform operations with the same dataflow, the number of cycles spent on an operation within a pPIM cluster is unaffected by the ISA. The ISA also has a smaller delay than that of

the pPIM clusters. With the proposed ISA the pPIM clusters are capable of operating at its fastest possible clock speed. This allowed the impact on throughput within the pPIM column to be minimized.

The added area overhead has a negligible effect on the overall pPIM architecture. This is due to the small percentage of the pPIM column that is allocated for the ISA. Approximately 0.0029% of the pPIM architecture's area is dedicated to the ISA.

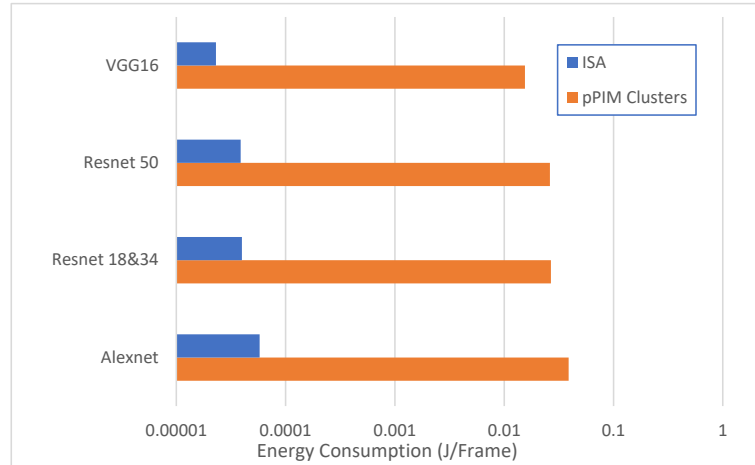


**Figure 4.7:** Comparison of power consumption of the ISA and pPIM clusters in various deep learning models.

A measure of the power consumption of both the ISA and the pPIM processing elements is run on Alexnet, Resnet 18, Resnet 34, Resnet 50, and VGG16. The results from the comparison are shown in Figure 4.7. The power consumption of the ISA is several decades below that of the pPIM clusters for each of the deep learning models. Due to the low power consumption of the ISA the energy of the pPIM architecture has a negligible decrease.

The throughput and energy efficiency of the ISA-driven pPIM architecture is measured on Alexnet. The modeling is done through analysis of the delay of the synthesized models when performing MAC operations. The throughput is compared at the 28nm technology node to KNL, Intel Neural Stick, Nvidia Tesla P100, and AI accelerators Edge TPU, as well as contemporary PIM architectures, LAcc and DRISA.

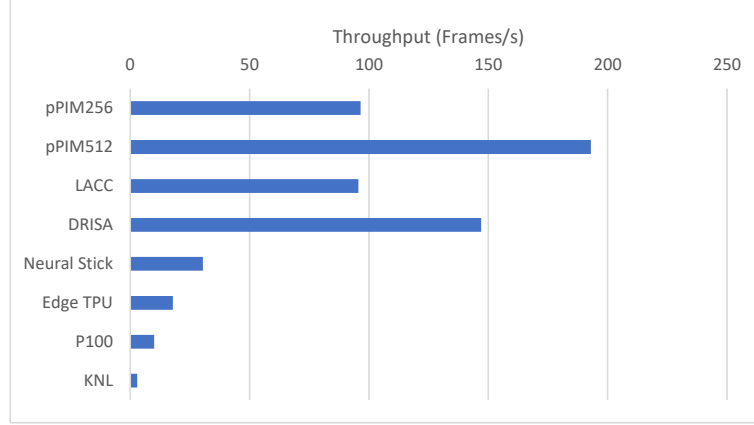


**Figure 4.8:** Comparison of throughput for inference on Alexnet.

Figure 4.8 displays the results of the throughput comparisons. With the added overhead of the ISA, the pPIM architecture delivers a highly competitive throughput. DRISA is capable of outperforming the pPIM 256-cluster configuration, however, the pPIM 512-cluster configuration outperforms DRISA. Both of the pPIM configurations outperform LACC in throughput. This is likely due to the decomposition of MAC operations into 4-bit operand functions. This reduces the size of LUTs that are required and improves throughput.

#### 4.6.2 FPGA Characteristics

**Table 4.3:** Synthesis results for FPGA implementation of pPIM ISA

Component	Power (W)
Clocks	0.033
Signals	0.003
Logic	0.002
BRAM	0.004
MMCM	0.122
Inputs/Outputs	0.001

The resulting FPGA implementation of the pPIM ISA is capable of correctly performing unsigned 8-bit MAC operations at a clock frequency of 75MHz. While the clock frequency of the pPIM architecture operates at 75MHz, the design is ultimately



limited by the UART communication. Since each instruction is capable of performing a single MAC operation on each cluster, the bottleneck in the computation is between the time to communicate the instruction and the actual computation. With a baudrate of 115200 baud/s, 3840 instructions can be communicated per second. The pPIM implementation operates faster than this with a speed of 16667 MAC operations that can be computed per second.

Reports on the power consumption of the implementation were gathered on Vivado. The measurements on power consumption of the design are recorded in Table ???. Without the inclusion of the PS in the FPGA implementation, the power consumption of the pPIM architecture dropped drastically to a power consumption of 0.163W.

## Chapter 5

---

### Conclusions & Future Work

The growing divide between processing and memory architecture is driving the need for high-performance architectures that reduce the penalties incurred by memory access. Processing-in-memory (PIM) architectures take a step away from traditional computer architectures by adding processing elements into memory and reducing the memory access. The programmable PIM architecture delivers high-performance processing while remaining reprogrammable to adapt to various applications. This is accomplished through the use of LUT-based multiplexers that are capable of being programmed to suit various functions and larger operations when processing in unison. Compared to contemporary PIM architectures, the pPIM delivers competitive throughputs with the highest level of efficiency for area and power consumptions.

An Instruction ISA is proposed for enabling the processing of data-intensive applications on the pPIM architecture. Through the use of a micro-coded approach to handling the control signals of the pPIM architecture, the ISA is capable of executing any operation that is compatible with the pPIM architecture. The ISA is capable running without hindering the performance of the pPIM architecture, with low impact on the area overhead and power consumption.

Additionally a proof-of-concept, an FPGA model of the pPIM architecture is designed for classification of images. The model implemented on the FPGA is a single layer Neural Network (NN) that classified MINST images with a prediction of

the digit within the image. The implementation is capable of correctly classifying images at a clock frequency of 200 MHz.

## **5.1 Future Work**

The presented work delivers synthesized models for a PIM architecture and its ISA. Additional steps are needed to further integration for programmers. These steps include the development of a compiler and developing libraries that are capable of executing deep learning models on the pPIM architecture. The work also focuses on the use of the pPIM architecture for deep learning applications. Further work is needed to display the pPIM architecture's ability to adapt to applications. This includes developing applications such as encryption and encoding on the pPIM architecture.

The work presented on the proof-of-concept only tests the processing elements of the pPIM architecture in a single layer NN. Research is needed into finding FPGAs that will have a higher capacity to represent an entire 8-cluster pPIM column. The pPIM architecture also needs to be proven to perform more complex machine learning models. This requires that an FPGA implementation performs machine learning models such as Alexnet and Resnet.

# Bibliography

---

- [1] S. McKee, “Reflections on the memory wall,” 2004.
- [2] G. S. et al, “A review of near-memory computing architectures: Opportunities and challenges,” 2018.
- [3] D. Patterson, “A case for intelligent ram,” 1997.
- [4] M. Wulf and S. McKee, “Hitting the memory wall: Implications of the obvious,” 1994.
- [5] V. S. et al, “Rowclone: Fast and energy-efficient in-dram bulk data copy and initialization,” 2013.
- [6] —, “Buddy-ram: Improving the performance and efficiency of bulk bitwise operations using dram,” 2016.
- [7] —, “Ambit: In-memory accelerator for bulk bitwise operations using commodity dram technology,” 2017.
- [8] Q. D. et al, “Lacc: Exploiting lookup table-based fast and accurate vector multiplication in dram-based cnn accelerator,” 2019.
- [9] J. S. et al, “Lupis: Latch-up based ultra efficient processing in-memory system,” 2018.
- [10] S. Li, “Drisa: A dram-based reconfigurable in-situ accelerator,” 2017.
- [11] Q. Deng, “Dracc: a dram based accelerator for accurate cnn inference,” 2018.
- [12] P. C. et al, “Prime: A novel processing-in-memory architecture for neural network computation in rram-based main memory.”
- [13] P. S. et al, “ppim: A programmable processor-in-memory architecture with precision-scaling for deep learning,” 2020.
- [14] A. Bear, “A novel processing-in-memory architecture for dense and sparse matrix multiplications,” 2019.
- [15] W. J. L. et al, “Design of processing-’inside’-memory optimized for dram behaviors,” 2019.
- [16] M. K. et al, “Software platform dedicated for in-memory computing circuit evaluation,” 2020.
- [17] —, “Smart instruction codes for in-memory computing architectures compatible with standard sram interfaces,” 2018.

- [18] “Hmc-mac: Processing-in memory architecture for multiply-accumulate operations with hybrid memory cube,” 2018.
- [19] P. Sutradhar, “A review of in-memory computing architectures for machine learning applications,” 2020.
- [20] K. C. et al, “Low-cost inter-linked subarrays (lisa): Enabling fast inter-subarray data movement in dram,” 2016.

**Table 1:** List of Publications and Submissions on pPIM Architecture

Article	Status	Venue
pPIM: A Programmable Processor-in-Memory Architecture with Precision-Scaling for Deep Learning	Computer Architecture Letters	Published
Look-up-Table based Processing-in-Memory Architecture with Programmable Precision-Scaling for Deep Learning Applications	Transactions on Parallel and Distributed Systems	Published on Early Access
Instruction Set Architecture for Programmable Processing-in-Memory Architecture with Deep Learning Applications	Under Blind Review	Submitted